Robotics and Computer-Integrated Manufacturing 29 (2013) 1–7

Contents lists available at SciVerse ScienceDirect

Robotics and Computer-Integrated Manufacturing

journal homepage: www.elsevier.com/locate/rcim

Review

PM based multi-component F/T sensors—State of the art and trends

Qiaokang Liang [a,*], Dan Zhang [b], Yaonan Wang [a], Gianmarc Coppola [b], Yunjian Ge [c]

[a] College of Electrical and Information Engineering, Hunan University, Changsha, Hunan 410082, China
[b] Faculty of Engineering and Applied Science, University of Ontario Institute of Technology, Oshawa, ON, Canada, L1H 7K4
[c] Institute of Intelligent Machines, Chinese Academy of Sciences, Hefei, Anhui 230031, China

ARTICLE INFO

Article history:
Received 27 August 2012
Received in revised form
30 November 2012
Accepted 4 December 2012
Available online 20 January 2013

Keywords:
Sensors
Force
Torque
Parallel
Calibration

ABSTRACT

Recent advancement in force/torque (F/T) sensor technologies have been powered by new measurement principles, novel structures of elastic elements (EEs), advanced manufacturing technologies, nonlinear signal processing and decoupling algorithms using artificial intelligence. The interlocked interaction of novel advances in these areas provide promising solutions improving the static and dynamic performances such as sensitivity, accuracy, compactness, economic efficiency, stiffness, and resonant frequency of F/T sensors.

A detailed overview on the current selected solutions for significant developments of measurement principles, EE structures, manufacturing technologies, signal processing and decoupling methods characterizing recently F/T sensors. In addition, several predominantly development trends in the future are presented.

Contents

1. Introduction

Multi-component F/T sensors have played a vital role in controlling robots in contact with the unknown or changing environment in automatic and industrial robotic applications. After force/torque control has been recognized as a key scheme [1], various types of multi-component F/T sensors have been developed [2–5]. Several high-precision six-component F/T sensors, such as ATI Nano17 and JR^3 50M31A, are commercially available at present. To keep up with the requirements of permanent enhancement of quality and reliability, the development of F/T sensors is required to provide cutting-edge approaches and solutions profiting from recent developments in science and technology [6].

Generally, multi-component F/T sensors achieve their function through a synergetic interaction of EE structure, manufacturing technology, signal processing and decoupling method. Consequently, the advancements of multi-component F/T sensor are

* Corresponding author.
E-mail address: qiaokang@mail.ustc.edu.cn (Q. Liang).

0736-5845/$ - see front matter © 2012 Elsevier Ltd. All rights reserved.
http://dx.doi.org/10.1016/j.rcim.2012.12.002

based on the substantial technical progress in these fields, as shown in Fig. 1. Recently, essential improvements are carried out in these fields involving a potential for novel approaches of multi-component F/T sensor.

2. Multi-disciplinary measurement principles

Generally, the measurement chain of a structure of a multi-component F/T sensor consists of several elements from true load to measured F/T, as shown in Fig. 2. The load (F and/or T) acts on the EE of the sensor, and the physic change (displacement, strain, potential, etc.) occurred on EE is converted into the electric quantity by the measuring element and the measure circuit. The voltage changes because the measuring circuit are generally tiny (measured in micro-volts), hence some incorporated electronics such as instrumentation amplifiers are used. Modern instrumentations use the digital measurement and analog-to-digital converters (ADCs) to perform A/D conversion nearer to the measuring circuit [7]. Based on specific algorithms and using special application programs, digital signal processing functions such as filtering, temperature compensation, creep correction are performed by the micro-computer or PC.

In order to convert multi-component force/torque into electrical signals, several measurement techniques such as resistive (SGs and piezoresistive), capacitive, inductive, optical, piezoelectric, magnetostrictive principles are used. The main features of a selection of multi-component F/T sensors and the measurement methods used are summarized in Table 1.

The transduction methods which have received most attention in F/T sensors design are concerned with the resistive and capacitive approaches. The most popular and extremely effective element in the former approach remains as the electrical resistance strain gauge, which experience a change in resistance when they are strained on special EEs [8–13]. Capacitors (in parallel, cylindrical, and spherical configurations) are the heart of the capacitive-sensing F/T sensors, which always consist of several electrodes and capable of changing its capacitance in accordance to the applied F/T. Generally, advantages of such capacitive F/T sensors are their extremely high sensitivity and resolution, compactness, resistance to severe environments (radiation and magnetic fields), vibration, and high bandwidth but they are temperature sensitive [14–17].

Fig. 1. Possible fields for the new generation of F/T sensors.

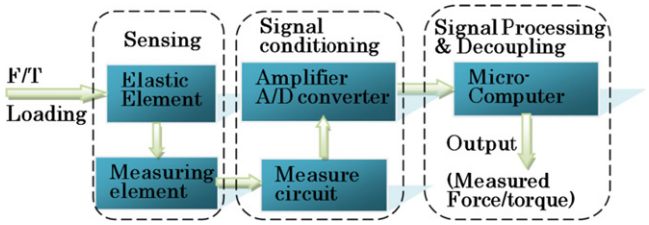

Fig. 2. General structure of a multi-component F/T sensor measurement chain.

Optical multi-component F/T sensors, which can be assembled by photo sensor and integrating light source (LED, laser diode, etc.), have significant advantages compared to conventional sensors, in terms of their properties such as electrical passiveness, freedom from electromagnetic interference, and wide dynamic range [18–22].

By using direct piezoelectric effect [23], the piezoelectric multi-component F/T sensor is the better choice for measuring dynamic F/T while the others are more suitable for static F/T. Another impressive advantage of piezoelectric F/T sensor is the wild measurement range extended from milli- to mega-Newtons [24–28]. Over past two decades, several advances have been made in piezoelectric MEMS sensors, and a need for the integration of piezoelectric materials into micro-machined sensors has emerged [28].

Magnetostrictive force sensors utilize Villari effect (Joule effect) that relates the change in permeability of a metal to the strain applied to the material to determine the force [29–32]. The primary disadvantage with magnetostrictive force sensor is the lack of knowledge of the material throughout the temperature range.

3. PM based EEs structure

Many different structures have been conceived as EEs of multi-component F/T sensors. Generally, they perform well for most applications. However, traditional multi-component F/T sensors suffer one very critical drawback—the trade-off among its various parameters such as sensitivity and stiffness. Additionally, another major disadvantage of the traditional multi-component F/T sensors is the coupling among components [33,34]. Moreover, because there are several components to be measured simultaneously, measurement isotropy among components is desired.

Parallel mechanisms (PM) are considered as an excellent candidate for the EEs of a multi-component F/T sensor due to their following advantages:

(i) Mature theory system: theories such as stiffness analysis, dynamics have been investigated for a long time and is well known;
(ii) Providing de-coupling F/T information: unlike traditional EEs that sense the all F/T components with a single monolithic structure, PM based EEs employ their limbs to sense the components;
(iii) Measurement isotropy: the global stiffness matrix denoting the relationship between the undergoing load and the infinitesimal movement of the mobile platform can be obtained and used to pursue measurement isotropy among components based on the statics analysis of PM;
(iv) Coexistence of high stiffness with high sensitivity: the traditional EEs with high stiffness always suffer from low sensitivity [35,36]. On the contrary, for the PM based EEs, the limb stiffness can be much lower compared to the overall required stiffness of the sensor due to their parallel arrangement.

Table 1
Comparisons on principal multi-component F/T sensors.

Device	Effect	Macroscopic Descriptions	Size & no. of axes	F/T range & sensitivity
Mastinu et al. [10,11]	Resistive	Three-spoke EE structure with sliding spherical joints, strain gauges	150 × 175 × 100 mm & 6	10 kN, 0.5 kN m & 0.003 μV/N, 5.03 μV/N m
Tibrewala et al. [13]	Piezoresistive MEMS	Membrane with p-type piezoresistors	6.5 × 6.5 × 0.25 mm & 3	n.a. & 0.37–0.39 mV/(V mN) in *Z*, 1.68–2.92 mV/(V mN) in *X* and *Y*
Zhu and Spronck [14]	Capacitive	Spatial sampling principle by measuring variation in the phase and amplitude of output signal.	8 mm (overlap in *Y* direction) & 3	10 N & 1 μm
Beyeler et al. [15]	Capacitive MEMS	Transverse sensing for seven capacitors, bulk silicon fabrication,	10 × 9 × 0.5 mm & 6	1000 μN, 2600 nN & 1.4 μN, 3.6 mN m
Ohka et al. [21]	Optical	Calculate force from integration and centroid displacement of the grayscale value	42.6 × 27 mm& 3	2 N & 0.43 mm/N
Liu et al. [25]	Piezoelectric	Piezoelectric quartz that square arranged in circle	Φ150/60 mm& 6	0.24 pC/Unit

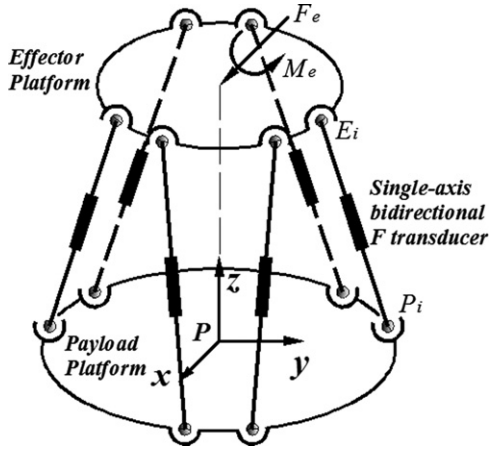

Fig. 3. Schematic diagram of the six-component F/T sensor based on Stewart platform.

Therefore, the trade-off between stiffness and sensitivity can be solved.

Recently, some researchers developed force/torque sensors based on parallel mechanisms to meet the requirement and escape the mentioned shortcoming. Gailet and Reboulet designed a force sensor of Stewart platform based on octahedral structure [35]. Dwarakanath and Bhaumick developed and implemented a force/torque sensor based on the Stewart platform structure in 1999, and the analysis deals with kinematic design, leg design and optimization of the form of the leg and the aspects of integration was presented [36]. Ranganath et al. analyzed and designed a Stewart platform based force/torque sensor in a near-singular configuration, which can measure some of the six components with high sensitivity [37]. Nguyen et al. presented the kinematic analysis of a 6 DOF force/torque sensor based on the mechanism of the Stewart platform and composed of two platforms coupled together by 6 spring-loaded pistons [38]. Dasgupta et al. disclosed a design methodology for the Stewart platform sensor structure based on the optimal conditioning of the force transformation matrix [39].

As shown in Fig. 3, the structure of the F/T sensor based on Stewart platform in hexagonal arrangement [40] is composed of an effector platform, payload platform, and six legs with single-axis bidirectional force transducers, which connect the two platforms with spherical joints. Right-hand coordinate frame {***P***} is assigned to the payload platform, and the origin of frame is chosen to be the centroid P of the payload platform. To measure the external load {$\boldsymbol{F}_e$, $\boldsymbol{M}_e$} experienced by the centroid of the effector platform, the axial forces f_i produced on the legs are sensed. The equilibrium equation of the effector platform is formulated as following:

$$\boldsymbol{F}_e + \in \boldsymbol{M}_e = \sum_{i=1}^{6} f_i \$_i \tag{1}$$

where $\$_i$ is the unit screw along the *i*th leg, and could be obtained by

$$\$_i = \boldsymbol{S}_i + \in \boldsymbol{S}_{oi} \tag{2}$$

where

$$\boldsymbol{S}_i \boldsymbol{S}_i = 1, \quad \boldsymbol{S}_i \boldsymbol{S}_{oi} = 0 \tag{3}$$

From Fig. 3, one can obtain

$$\boldsymbol{S}_i = \frac{\boldsymbol{E}_i - \boldsymbol{P}_i}{|\boldsymbol{E}_i - \boldsymbol{P}_i|} \tag{4}$$

$$\boldsymbol{S}_{oi} = \boldsymbol{P}_i \boldsymbol{S}_i = \frac{\boldsymbol{P}_i \boldsymbol{E}_i}{|\boldsymbol{E}_i - \boldsymbol{P}_i|} \tag{5}$$

Eq. (1) can be rewritten in the form of matrix equation as

$$\boldsymbol{F} = [\boldsymbol{T}_f^F]\boldsymbol{f} \tag{6}$$

where

$$\boldsymbol{F} = \begin{bmatrix} \boldsymbol{F}_e^T & \boldsymbol{M}_e^T \end{bmatrix}^T = \begin{bmatrix} F_x & F_y & F_z & M_x & M_y & M_z \end{bmatrix}^T \tag{7}$$

$$\boldsymbol{f} = \begin{Bmatrix} f_1 & f_2 & f_3 & f_4 & f_5 & f_6 \end{Bmatrix}^T \tag{8}$$

$$\begin{aligned} \left[\boldsymbol{T}_f^F\right] &= \begin{bmatrix} \boldsymbol{S}_1 & \boldsymbol{S}_2 & \boldsymbol{S}_3 & \boldsymbol{S}_4 & \boldsymbol{S}_5 & \boldsymbol{S}_6 \\ \boldsymbol{S}_{o1} & \boldsymbol{S}_{o2} & \boldsymbol{S}_{o3} & \boldsymbol{S}_{o4} & \boldsymbol{S}_{o5} & \boldsymbol{S}_{o6} \end{bmatrix} \\ &= \begin{bmatrix} \frac{\boldsymbol{E}_1 - \boldsymbol{P}_1}{|\boldsymbol{E}_1 - \boldsymbol{P}_1|} & \cdots & \frac{\boldsymbol{E}_i - \boldsymbol{P}_i}{|\boldsymbol{E}_i - \boldsymbol{P}_i|} & \cdots & \frac{\boldsymbol{E}_6 - \boldsymbol{P}_6}{|\boldsymbol{E}_6 - \boldsymbol{P}_6|} \\ \frac{\boldsymbol{P}_1 \boldsymbol{E}_1}{|\boldsymbol{E}_1 - \boldsymbol{P}_1|} & \cdots & \frac{\boldsymbol{P}_i \boldsymbol{E}_i}{|\boldsymbol{E}_i - \boldsymbol{P}_i|} & \cdots & \frac{\boldsymbol{P}_6 \boldsymbol{E}_6}{|\boldsymbol{E}_6 - \boldsymbol{P}_6|} \end{bmatrix} \end{aligned} \tag{9}$$

The condition number [41,42], which could ascertain the isotropic quality, is defined as

$$I_s = \|\boldsymbol{T}_f^F\| \left\| \left(\boldsymbol{T}_f^F\right)^{-1} \right\| \tag{10}$$

And the norm of a square matrix is given by

$$\|\boldsymbol{T}_f^F\| = \sqrt{Tr\left(\boldsymbol{T}_f^F D\left(\boldsymbol{T}_f^F\right)^{-1}\right)} \tag{11}$$

where $\boldsymbol{D}=1/6\boldsymbol{I}_{6\times 6}$.

The stiffness of F/T sensors based on PMs is dependent on the force transducers in legs, the structures and materials of the legs, the topologies and the geometries of structures, the payload platform stiffness and effector platform stiffness. As the stiffness of the force transducer is weaker than other elements in the system, the general stiffness model for F/T sensors based on PM is always proposed in consideration of the influence of the transducers stiff. Stiffness matrix relates the forces and torques applied on the effector platform to the corresponding displacements of legs. Jacobian matrix $\boldsymbol{J}$ is the mapping from the Cartesian vector (Cartesian infinitesimal displacement $\delta\boldsymbol{x}$) to the joint velocity vector (legs displacement $\delta\boldsymbol{q}$).

$$\delta\boldsymbol{q}=\boldsymbol{J}\delta\boldsymbol{x} \tag{12}$$

The forces and displacement occur on legs can be related by

$$\boldsymbol{f}=\boldsymbol{K}\delta\boldsymbol{q} \tag{13}$$

where $\boldsymbol{K}$ is the transducer stiffness matrix of the force transducer

$$\boldsymbol{K}=diag[k_1,\ldots,k_n] \tag{14}$$

and k_i is a scalar representing the transducer stiffness of each leg. Substituting Eq. (12) to Eq. (13), yields

$$\boldsymbol{f}=\boldsymbol{K}\boldsymbol{J}\delta\boldsymbol{x} \tag{15}$$

Then, substituting Eq. (15) into Eq. (6), yields

$$\boldsymbol{F}=[\boldsymbol{T}_f^F]\boldsymbol{K}\boldsymbol{J}\delta\boldsymbol{x} \tag{16}$$

As there is a relationship between $\boldsymbol{J}$ and $[\boldsymbol{T}_f^F]$

$$[\boldsymbol{T}_f^F]=\boldsymbol{J}^T \tag{17}$$

Then,

$$\boldsymbol{F}=[\boldsymbol{T}_f^F]\boldsymbol{K}[\boldsymbol{T}_f^F]^T\delta\boldsymbol{x} \tag{18}$$

Hence, the stiffness matrix of the sensor in the Cartesian space is then given by the following expression:

$$\boldsymbol{K}_c=[\boldsymbol{T}_f^F]\boldsymbol{K}[\boldsymbol{T}_f^F]^T \tag{19}$$

The stiffness matrix's eigenvalues represent the coefficients of stiffness in the principal directions. Condition number, a measure of the dexterity of the mechanism, can be written as [43,44]

$$\frac{1}{c}=\sqrt{\varsigma_{\min}/\varsigma_{\max}} \tag{20}$$

where ς_{max} and ς_{min} respectively represent the largest and smallest eigenvalues of the stiffness matrix.

4. Signal transmission and processing

The main purpose of the signal transmission and processing of a PM based multi-component F/T sensor is to specify the measured quantity (Cartesian F/T components) from the measured data, which is in the range of tens of Millivolt and affected by influence factors (IFs) such as cross coupling, temperature drift, and null shift. The signal processing and electronic instrumentation associated with the sensor could be extremely complex. At present there are two frequently used measurement ways in PM based multi-component F/T sensors presently.

4.1. Integrative measurement systems

For reasons such as usability, safety, portability and low-cost, all electronic instrumentations and data processing components are integrated into a DSP/MCU based embedded system, and the system accomplishes almost all functions such as signal processing, calibration, calculation, and decoupling. Fig. 4(a) illustrates the signal processing by integrative systems. All data are stored inside the sensor, and calibration data is read from the memory and installed into the instrumentation automatically. No large database, additional connectivity and computer are required. However, it is difficult to record and visualize the measurements and process the collected data for this type of system.

4.2. PC-based DAQ systems

As PCs and their applications continue to evolve and improve at a very fast pace, the signal transmission and processing is increasingly shifting from the hardware to software. Compared to integrative measurement systems, PC-based DAQ systems leverage as much of the personal or industry-standard computers' processing power, productivity, display, communication, and data storage capability as possible, and provide more powerful, versatile, expandable, economical to own, simple-to-use, and flexible measurement solutions.

A DAQ system for PM based multi-component F/T sensor comprises a sensor, DAQ measurement hardware, and a computer with programmable software. While few functions such as amplification are integrated into the transducer, most parts of the system are carried out by PC/DAQ that connects the transducer with standard interface bus. Fig. 4(b) shows block diagram of the signal transmission and processing for PC-based DAQ systems. The configuration of the sensor is simplified, even to a Wheatstone bridges with amplifications. DAQ hardware acts as the interface between the sensor and the PC and connects them over USB, Ethernet, or Wi-Fi. The PC with programmable software is used to retrieve the database information, control the operation of the DAQ device, and calculate, calibrate, visualize, and store measurement data.

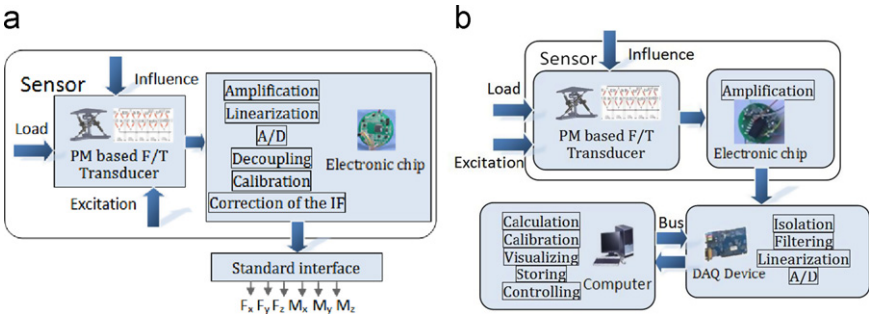

Fig. 4. Block diagram of the signal transmission and processing for integrative measurement system.

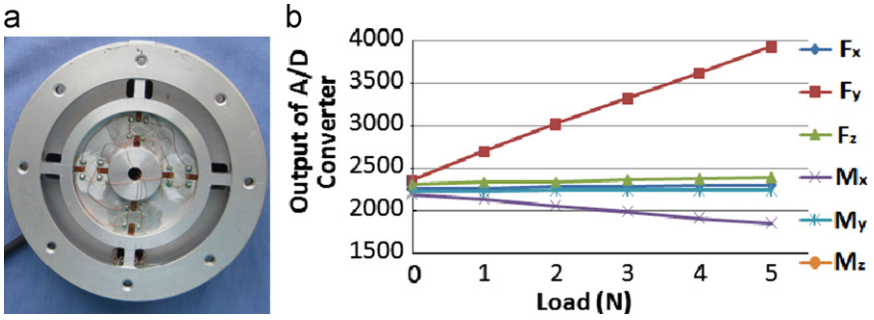

Fig. 5. Input–output curve (b) of a six-component F/T sensor (a) without decoupling.

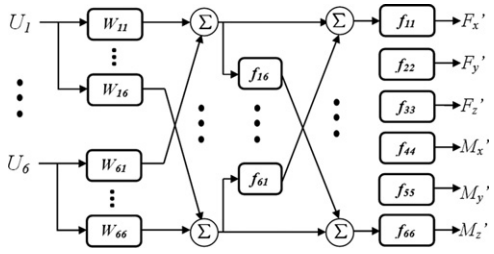

Fig. 6. Schematic representation of the static decoupling and calibration method.

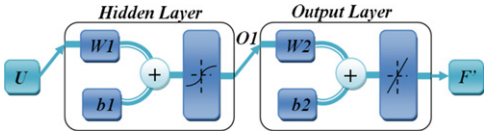

Fig. 7. Neural network model for decoupling and calibration.

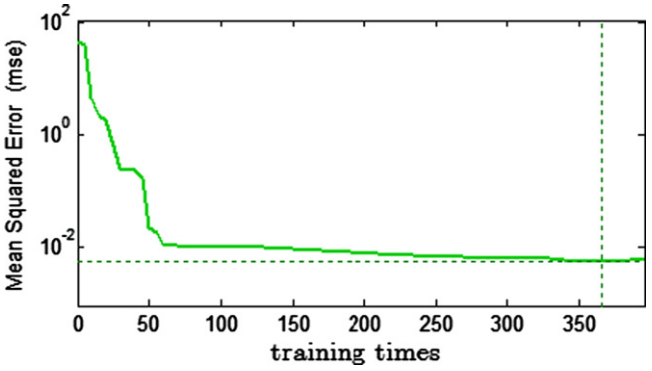

Fig. 8. Error curve of the neural network training.

5. Decoupling and calibration

Although the principles remain the same, the decoupling and calibration of PM-based multi-component F/T sensor is more demanding on the equipment, algorithm due to the existence of the specific cross coupling and influences such as machining error, joint frictional moment, and the assembling error. Cross coupling is the effect of a load along one axis that produces a change in output on other axes. Fig. 5 exhibits typical load-output curve of a six-component F/T sensor before decoupling process. It is obvious that component M_x occurs at an output due to the cross coupling when the sensor is subjected to the load F_y.

The decoupling methods for PM-based multi-component F/T sensor can be classified according to various criteria. One obvious classification scheme is to categorize the methods to digital and analog. The analog decoupling method utilizes analog amplifiers for each component and cross-couplings to pursue direct decoupling with more accurate performance, and no decoupling applications are required. While digital decoupling method applies A/D converters and specified decoupling applications to eliminate the effect of cross coupling. Another scheme is to classify the methods to static and dynamic according to their applied loads. Two general methods, excitation method and impact method, are adopted for dynamic calibration and decoupling [45–48]. The static decoupling and calibration method uses only the present output as feedback because it has no relationship with the previous output. As shown in Fig. 6, the input vector $\boldsymbol{U} = [U_1 \;\; U_2 \;\; U_3 \;\; U_4 \;\; U_5 \;\; U_6]^T$ is the output voltages of the sensitive bridge circuits, and the output vector $F' = [F^T \;\; M^T]^T = [F'_1 \;\; F'_2 \;\; F'_3 \;\; M'_4 \;\; M'_5 \;\; M'_6]^T$ are the outputs of the sensor after decoupling. $W_{ij} = a_{0ij} + a_{1ij}x + a_{2ij}x^2$ denotes the relationship between the output of component j due to the input of component i, and $f_{ij} = a_{0ij} + a_{1ij}x + a_{2ij}x^2 + \ldots + a_{nij}x^n$ is the decoupling transfer function. A relationship between the load and measured value can be obtained as

$$F'_i = f_{ii}\left(\sum_{j=1}^{6} W_{ji}U_j + \sum_{k\neq i} f_{ki}\left(\sum_{j=1}^{6} W_{jk}U_j\right)\right) \tag{21}$$

Eq. (21) represents the true nature of the PM-based multi-component F/T sensor, and it is available to solve the nonlinear cross coupling theoretically. But its low computational efficiency restricts its practicability. Recently, Artificial Neural Network (ANN) approaches are proposed to decouple and calibrate the PM-based multi-component F/T sensors. As shown in Fig. 7, a three-layer ANN with tan-sigmoid transfer in the hidden layer and a linear transfer function in the output layer is disclosed. The input vector and output vector are U and F' respectively, and the learning samples are a group of applied forces/torques and the corresponding outputs voltages of the circuits. The output corresponding to U may be expressed as

$$F' = purelin\{W_2[tansig(W_1U + b_1)] + b_2\} \tag{22}$$

where *purelin*( ) and *tansig*( ) represent linear transfer function and hyperbolic tangent sigmoid transfer function, respectively.

The number of neurons in hidden layer is determined by the experiment. For a general six-component F/T sensor, seven hidden layer neurons are rational to get appropriate convergence rate with uncomplicated structure. Fig. 8 shows the error curve of the ANN decoupling and calibration method for the sensor proposed in Ref. [9]. After 360 training times, MSE of the training is below 0.01. Other methods such as FLANN, Particle Swarm Algorithm, and support vector machine are drawing attractions as potential efficacious decoupling and calibration methods.

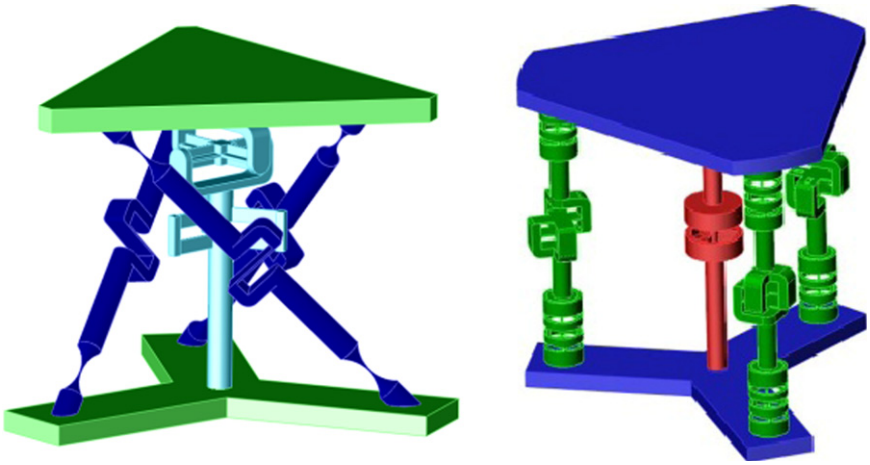

Fig. 9. Novel configurations for CPM based multi-component F/T sensors.

6. Future trends in PM based multi-component F/T sensors

Future trends in PM based multi-component F/T sensors result from specific and higher requirements, and wider application requests. Next generation of the PM based multi-component F/T sensor will be achieved by using new manufacturing technologies, applying novel structural configurations and measurement principles, and sophisticated signal processing methods.

6.1. Compliant Parallel Manipulator (CPM) based multi-component F/T sensors

The presence of clearance, backlash and friction at the rigid mechanical joints of PM will modify the axial forces that the sensing limbs undergo, consequently, disturb the performance of the sensor in unpredictable ways [49,50]. To avoid these problems, force-sensing candidate based on parallel mechanism is preferred to be designed with flexural joints, which eliminate the friction, backlash and wear and possess sub-micron accuracy with high resolution, continuous and smooth displacement [51].

Two configurations for CPM based multi-component F/T sensors are shown in Fig. 9. All rigid connections are replaced by novel flexure joints, which are also used as force-sensing elements. Measurement principles based on LVDT, strain gauges, capacitive, piezoelectric crystal, electromagnetic, magnetoelastic could be utilized to detect the applied force/torque. As the majority of micro-/nano-manipulators are in CPM configurations [52–54], CPM based F/T sensors provide the economical and compact advantage by integrating into the manipulator system with the same mechanism [55].

6.2. MEMS based multi-component F/T sensors

In less than 30 years, the breakthrough Micro Electro-Mechanical Systems (MEMS) technology has the potential to revolutionize many sensors by realizing the complete-system-on-a-chip [56,57]. Advances in IC technology and semiconductor fabrication process have been applied to multi-component F/T sensors, as 'micro-systems' or 'smart sensors', to measure forces as small as a few nano-Newtons with improved sensitivity in applications such as bio-chemistry and microtechnology. Measurement principles based on optical, piezoelectric crystal, and capacitive could be used. Generally, its elastic element and sensing element can be integrated into the MEMS structures.

As shown in Fig. 10, intended to characterize and quantify roughness of the polished or super finished surfaces, a potential

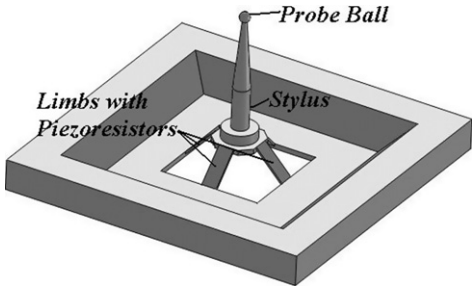

Fig. 10. Schematic view of a potential MEMS multi-component F/T sensor based on PM.

MEMS multi-component F/T sensor based on PM is designed using silicon micromachining technology. The innovative design of the probe system is based on a CPM structure with piezoresistors integrated into its limbs, which ensures that the system possesses good isotropy and high stiffness. Based on the relationship between the measured contact force vector and the geometric shape of the probe, the exact coordinates of the contact points are obtained. The proposed system could be used to investigate micromechanical structures with nanometer accuracy.

7. Conclusion

F/T sensor profits from the synergetic interaction of novel EEs structure designs, manufacturing technologies, signal processing and decoupling methods. The last achievements for the multi-component F/T sensor include the PM-based multi-component F/T sensors, which can significantly provide promising technical advantages such as measurement isotropy, high stiffness, and high sensitivity.

A brief overview about multi-component F/T sensors based on PM has been discussed in this paper. Fundamental methods and common technique in the field were proposed. The current research work and the trends of PM based multi-component F/T sensors were presented.

Acknowledgments

This research was supported by the National Nature Science Foundation of China (No. 61203207). The second author gratefully acknowledges the financial support from the Canada Research

Chairs Program, Early Researcher Award from Ministry of Research and Innovation of Ontario and the MITACS-NCE Research Project.

References

[1] Nakamura Y, Yoshikawa T, Futamata I., Design and signal processing of six-axis force sensors. In: Proceedings of the 4th international symposium of robotics research, Santa Barbara, CA, USA; 1987: p. 75–81.
[2] Kim G-S. Development of 6-axis force/moment sensor for a humanoid robot's foot. IET Science, Measurement and Technology 2008;2(3):122–33.
[3] Park Jae-jun, Kwon Kihwan, Cho Nahmgyoo. Development of a coordinate measuring machine (CMM) touch probe using a multi-axis force sensor. Measurement Science and Technology 2006;17:2380–6.
[4] Kim JH, Kang DI, Shin HH, Park YK. Design and analysis of a column type multi-component force/moment sensor. Measurement 2003;33:213–9.
[5] Kim. GS. The design of a six-component force/moment sensor and evaluation of its uncertainty. Measurement Science and Technology 2001;12(9): 1445–55.
[6] Liang Q, Zhang D, Ge Y, Song Q. A novel miniature four-dimensional force/torque sensor with overload protection mechanism. IEEE Sensors Journal 2009;9(12):1741–7.
[7] Fraden J. Handbook of modern sensors—physics, designs, and applications. 3rd edn New York: Springer-Verlag Inc; 2004.
[8] Liu SA, Tzo HL. A novel six-component force sensor of good measurement isotropy and sensitivities. Sensors and Actuators A: Physical 2002;100(2–3): 223–30.
[9] Liang Q, Zhang D, Ge Y, Huang X, Li Z. Miniature robust five-dimensional fingertip force/torque sensor with high performance. Measurement Science and Technology 2011;22(3):35205–15.
[10] Mastinu G, Gobbi M, Previati G. A new six-axis load cell. Part I: design. Experimental Mechanics 2011;51(3):373–88.
[11] Mastinu G, Gobbi M, Previati G. A new six-axis load cell. Part II: error analysis, construction and experimental assessment of performances. Experimental Mechanics 2011;51(3):389–99.
[12] Liang Q, Zhang D, Song Q, Ge Y. Design and fabrication of a six-D wrist force/torque sensor based on E-type membranes compared to cross beams. Measurement 2010;43(10):1702–19.
[13] Tibrewala A, Phataralaoha A, Büttgenbach S. Simulation, fabrication and characterization of a 3D piezoresistive force sensor. Sensors and Actuators A: Physical 2008;147(2):430–5.
[14] Zhu F, Spronck JW. A capacitive tactile sensor for shear and normal force measurements. Sensors and Actuators A: Physical 1992;31(1–3):115–20.
[15] Beyeler F, Muntwyler Simon, Bradley J. Nelson. A six-axis MEMS force–torque sensor with micro-Newton and nano-Newtonmeter resolution. Journal of Micro-electromechanical Systems 2009;18(2):433–41.
[16] Sun Y, Nelson BJ. MEMS capacitive force sensors for cellular and flight biomechanics. Biomedical Materials 2007;2(1):16–22.
[17] Beyeler F, Muntwyler S, Nagy Z, Graetzel C, Moser M, Nelson BJ. Design and calibration of a MEMS sensor for measuring force and torque acting on a magnetic microrobot. Journal of Micromechanics and Microengineering 2008;18(2):025 004.
[18] Tada M, Sasaki S, Oeasawara T. Development of an optical force sensor usable in MRI environments. Proceedings of the IEEE Sensors 2002;64:4.
[19] Su Hao, Fischer GS. A 3-axis optical force/torque sensor for prostate needle placement in magnetic resonance imaging environments. In: Proceedings of the IEEE international conference on technologies for practical robot applications 2009, TePRA 2009, 9–10 November 2009, p. 5–9.
[20] Takahashi N, Tada M, Ueda J, Matsumoto Y, Ogasawara T. An optical 6-axis force sensor for brain function analysis using fMRI. Proceedings of the IEEE Sensors 2003;1:253–8.
[21] Ohka M, Mitsuya Y, Higashioka I. An experimental optical three-axis tactile sensor for micro-robots,. Robotica 2005;23(4):457–65.
[22] Ohka Masahiro, Kobayashi Hiroaki, Takata Jumpei, Mitsuya Yasunaga. An experimental optical three-axis tactile sensor featured with hemispherical surface. Journal of Advanced Mechanical Design, Systems, and Manufacturing 2008;2(5):860–73.
[23] Lee C, Itoh T, Suga T. Micromachined piezoelectric force sensors based on PZT thin films. IEEE Transactions on Ultrasonics, Ferroelectrics and Frequency Control 1996;43(4):553–9.
[24] Fan K, Song M, Lu R., Design and calibration of a novel piezoelectric six-axis force/torque sensor. In: Proceedings of the seventh international symposium on precision engineering measurements and instrumentation, vol. 8321.
[25] Liu W, Li Y, Jia Z, Zhang J, Qian M. Research on parallel load sharing principle of piezoelectric six-dimensional heavy force/torque sensor. Mechanical Systems and Signal Processing 2011;25(1):331–43.
[26] Li Y, Sun B, Zhang J, Qian M, Jia Z. A novel parallel piezoelectric six-axis heavy force/torque sensor. Measurement 2009;42(5):730–6.
[27] Li Y, Zhang J, Jia Z, Qian M, Li H. Research on force-sensing element's spatial arrangement of piezoelectric six-component force/torque sensor. Mechanical Systems and Signal Processing 2009;23(8):2687–98.
[28] Tadigadapa S, Mateti K. Piezoelectric MEMS sensors: state-of-the-art and perspectives. Measurement Science and Technology 2009;20(9):1–31.
[29] Baudendistel TA., Development of a novel magnetostrictive force sensor. PhD dissertation, University of Dayton, Dayton, OH, 2005.
[30] Schroeder T, Morelli DT. Magnetic force sensor and control circuit for the same. United States Patent Application 20040211268, October 28, 2004.
[31] Tayalia Prakriti, Heider Dirk, Gillespie John W. Characterization and theoretical modeling of MS strain sensors. Sensors and Actuators A 2004;111:267–74.
[32] Baudendistel T. Magnetostrictive strain sensor with hall effect, United States Patent 6931940, August 23, 2005.
[33] Liang Q, Zhang D, Song Q, Ge Y. A novel thin six-dimensional wrist force/moment sensor for underwater manipulators, Transactions of the North American Manufacturing Research Institution/SME, 2010; 38: 703–710.
[34] Frigola R, Ros L, Rource F, Thomas F. A wrench-sensitive touch pad based on a parallel structure. In: Proceedings of ICRA, 2008, p. 3449–54.
[35] Gailler A, Reboulet C. An isostatic six component force and torque sensor. In: Proceedings of the 13th international symposium on industrial robotics, 1983.
[36] Dwarakanath TA, Bhaumick TK, Venkatesh D. Implementation of Stewart platform based force–torque sensor. In: Proceedings of the IEEE/SICE/RSJ international conference on multisensor fusion and integration for intelligent systems, 1999, p. 32–7.
[37] Ranganath R, Nair PS, Mruthyunjaya TS, Ghosal A. A force-torque sensor based on a Stewart platform in a near-singular configuration. Mechanism and Machine Theory 2004;39:971–98.
[38] Nguyen C, Antrazi S, Zhou Z. Analysis and implementation of a 6-dof Stewart platform-based force sensor for passive compliant robotic assembly. In: Proceedings of the IEEE SOUTHEASTCON, 1991, p. 880–4.
[39] Dwarkanath TA, Dasgupta B, Mmruthyunjaya TS. Design and development of a Stewart platform based force–torque sensor. Mechatronics 2001;11: 793–809.
[40] Stewart DA. Platform with six degrees of freedom. Proceedings of the Institution of Mechanical Engineers 1965;1(80):371–86.
[41] Uchiyama M, Hakomori K. A few considerations on structure design of force sensors. In: Proceedings of the 3rd annual conference of Japan robotics society, 1985, p.17–8.
[42] Bicchi Antonio. A criterion for optimal design of multi-axis force sensors. Robotics and Autonomous Systems 1992;10(4):269–86.
[43] Gosselin CM. Stiffness mapping for parallel manipulators. IEEE Transactions on Robotics and Automation 1990;6(3):377–82.
[44] Dan Zhang, Gosselin M. Kinetostatic analysis and design optimization of the tricept machine tool family. ASME Journal of Manufacturing Science and Engineering 2002;124(3):725–33.
[45] Schmidt PA, Maël E, Würtz RP. A sensor for dynamic tactile information with applications in human–robot interaction and object exploration. Robotics and Autonomous Systems 2006;54(12):1005–14.
[46] Ferraresi C, Pastorelli S. Static and dynamic behavior of a high stiffness Stewart platform-based force/torque sensor. Journal of Robotic Systems 1995;12:883–93.
[47] Jingzhu Z, Kai G, Cheng X. Application study on static decoupling algorithms for six-dimensional force sensor. Transducer and Microsystems Technologies 2007;26(12):58–62.
[48] Xu Ke-Jun, Li Cheng. Dynamic decoupling and compensating methods of multi-axis force sensors. IEEE Transactions on Instrumentation and Measurement 2000;49(5):935–41.
[49] Moon YM, Kota S. Design of compliant parallel kinematic machines. In: Proceedings of ASME DETC'02, 2002, DETC2002/MECH-34204.
[50] Yi B-J, Chung GB, Na HY, Kim WK, Suh IH. Design and experiment of a 3-dof parallel micromechanism utilizing flexure hinges. IEEE Transactions on Robotics and Automation 2003;19(4):604–12.
[51] Trease BP, Moon YM, Kota S. Design of large-displacement compliant joints. ASME Journal of Mechanical Design 2005;127:788–98.
[52] Lee KM, Arjunan S. A three-degree-of-freedom micromotion in-parallel actuated manipulator. IEEE Transactions on Robotics and Automation 1991;7(5):634–41.
[53] Koseki Y, Tanikawa T, Koyachi N, Ari T., Kinematic analysis of translational 3-DOF micro parallel mechanism using matrix method. In: Proceedings of IEEE/RSJ international conference on intelligent robots and systems, 2000, p. 786–92.
[54] Liang Q, Zhang D, Chi Z, Song Q, Ge Y, Ge Y. Six-DOF micro-manipulator based on compliant parallel mechanism with integrated force sensor. Robotics and Computer-Integrated Manufacturing 2011;27:124–34.
[55] Tibrewala A, Hofmann N, Phataralaoha A, Jäger G, Büttgenbach S. Development of 3D force sensors for nanopositioning and nanomeasuring machine. Sensors 2009;9(5):3228–39.
[56] Stefanescu DM. Handbook of force transducers: principles and components. Heidelberg: Springer; 2011.
[57] Cullinan MA, Panas RM, Culpepper ML. Design and fabrication of a multi-axis MEMS force sensor with integrated carbon nanotube based piezoresistors. Nanotechnology 2011;2:302–5.